



Bachelor Thesis Technical Medicine
Multidisciplinary Assignment

CHANGE IN 3D PERIARTICULAR BONE DENSITY AFTER
KNEE JOINT DISTRACTION OR HIGH TIBIAL OSTEOTOMY
IN THE TREATMENT OF OSTEOARTHRITIS

Authors:

N. A. Coorens s1452789

C. J. Ensink s1245449

J. W. van der Graaf s1760599

B. Schippers s1448404

Supervisors:

Prof. Dr. C. H. Slump

MSc. N. J. Besselink

Dr. S. C. Mastbergen

Dr. P. de Jong

Enschede, 20th June, 2016

Abstract

Background: Osteoarthritis (OA) is a degenerative joint disease, associated with both cartilage and periarticular bone change. High Tibial Osteotomy (HTO) is a generally considered method for prolonging the time before a total knee replacement is necessary and to reduce the pain in patients suffering from OA. A relatively new technique is Knee Joint Distraction (KJD). Although there is evidence for an improvement of cartilage after KJD, changes in periarticular bone have not yet been investigated.

Objective: The main goal of this research is to determine the difference in quality of periarticular bone of the tibia before and two years after treatment with KJD or HTO using 3D Computed Tomography (CT).

Methods: Coronal CT images were obtained from two previous conducted studies, a total of 23 patients (mean age 51 ± 7 years; 15 males, 10 KJD) were included. Changes in bone density are related to changes in intensity, measured in Hounsfield Units (HU). In the assessment of the periarticular bone quality, a distinction was made between subchondral and trabecular bone, by calculating intensities in five different layers to a depth of 5 mm beneath the joint surface of the tibia. Bone quality was expressed in mean absolute deviation (MAD) and mean intensity.

Results: Mean intensities seem to be decreased at two year follow up compared to baseline, but these differences were statistically insignificant in both HTO and KJD. Interestingly, in the case of KJD, the MAD of the intensities in all layers of the lateral compartment and some layers of the medial and other compartments, were significantly decreased.

Conclusions: The results suggest that periarticular bone density neutralizes. This was statistically indistinguishable for HTO, but MAD decreased significantly for KJD. This indicates that joint distraction has a positive effect on the quality of periarticular bone.

Preface

Before you lies the thesis that we made as a completion of the bachelor and premaster in Technical Medicine at the University of Twente. It is a reflection of the competences and an opportunity to show the knowledge we acquired during the past years.

We have gained more experience in using software like LaTeX, SPSS and especially Matlab. We cheered and raised our hands in the air when Matlab showed us what we wanted it to show, but we execrated it when the red lines popped up for the umpteenth time.

To us, performing this research was an interesting challenge, in which we have felt delighted, as well as disheartened. But: “If the job was easy, there should be no need of the technical medical profession.” We would like to thank Cees Slump for this insight and many more he gave us during the process. Another thanks to Mattiënne van der Kamp for keeping an eye on the process and guiding our personal and professional development. Furthermore we would like to thank our supervisors from the UMC Utrecht for their supervision and contribution in this project. Special thanks to Nick Besselink, who was always available and willing to guide and support us during these ten weeks.

Nadine Coorens

Carmen Ensink

Jasper van der Graaf

Bas Schippers

Contents

Abstract	i
Preface	ii
1 Introduction	1
1.1 Osteoarthritis	1
1.2 Treatments	1
1.3 Study goal	2
2 Methodology	3
2.1 Computed Tomography	3
2.2 Subjects	3
2.3 Data Collection	4
2.4 Data Processing	4
2.4.1 Load DICOM files	4
2.4.2 Segmentation	4
2.4.3 Splitting tibia and femur	5
2.4.4 Intensity and location of tibial plateau	5
2.4.5 Reconstruction	6
2.5 Measurements and Calculations	6
2.6 Statistics	7
3 Results	8
3.1 Mean intensity outcome	8
3.2 Mean Absolute Deviation outcome	8
4 Discussion	11
4.1 Computed Tomography settings	11
4.2 Future recommendations	12
4.2.1 Partial volume effect	12
4.2.2 Ultra thin slices	12
4.2.3 Segmentation	13
4.3 Conclusion	13
References	14
 <i>Appendices</i>	
I Flowchart Methodology	A1
II List of Matlab Commands	A2
III Matlab Script	A3

1 Introduction

1.1 Osteoarthritis

Osteoarthritis (OA) is one of the most common disabling diseases in developed countries. World-wide, the prevalence of OA is estimated to be 9.6% for men and 18.0% for women aged over 60 years.^[1] OA can have effect on various different joints, but knee OA is most commonly seen.^[2]

OA is a degenerative joint disease, which is characterized by progressive degeneration of cartilage, subchondral sclerosis, osteophyte formation, changes in periarticular structures and joint inflammation, as shown in figure 1.^[3] These changes often lead to pain, stiffness and reduced mobility of the joint. The main cause of OA is still unclear, but there is evidence that biomechanical changes lead to damaged cartilage and bone, deteriorating the joint and inducing OA.^[4] It is believed that this process is counteracted by the formation of osteophytes which try to restore mechanical load within the joint.^[5]

Periarticular bone is composed of subchondral and trabecular bone. In OA, the formation of osteophytes and cysts can be found in the subchondral bone and trabecular bone. Subchondral bone thickness in the knee joint can vary from approximately 0.1 – 1.5 millimeter, where maxima can be seen at the central zones of the tibia and minima at the peripheral zones.^[6]

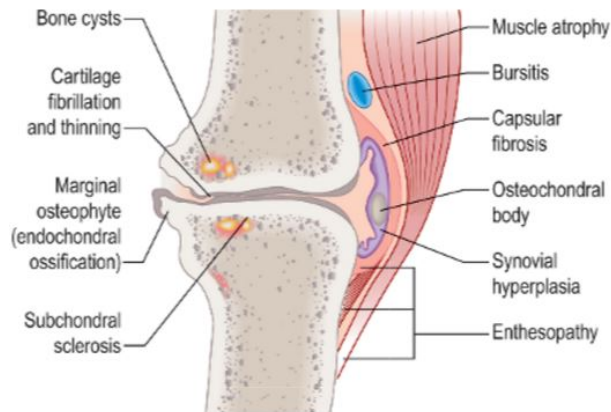


Figure 1: Schematic illustration of changes in osteoarthritis.^[7]

1.2 Treatments

Because OA still is an incurable disease, treatment focuses on reducing the symptoms. This is mainly done by reducing the load on the knee, physiotherapy and painkilling.^[8] If these options do not improve the circumstances sufficiently, surgery could be another possibility. High Tibial Osteotomy (HTO) relieves the pressure on the affected side of the knee by correcting the angle between the femur and tibia. This procedure is usually done if the medial side of the knee is affected by OA. An HTO can be done by the medial opening wedge or the lateral closing wedge technique. With both approaches the load on the medial side decreases while the load increases on the lateral side of the knee joint. In this way, the stress on the affected side is reduced.^[9]

A relatively new treatment is Knee Joint Distraction (KJD). In this surgical procedure the knee is externally fixated and distracted by a few millimeters.^[10] This distraction changes the pressure in the knee and takes the load of the cartilage and the periarticular bone tissue. These factors have shown to be critical for recovering of cartilage and bone tissue.^[11] However, it is not

well understood how these principles exactly work.^[12] The aim of both HTO and KJD, especially in relatively young patients, is to reduce the pain and stiffness related to OA and postpone the placement of a prosthetic knee, which is the final option to treat OA.^[10]

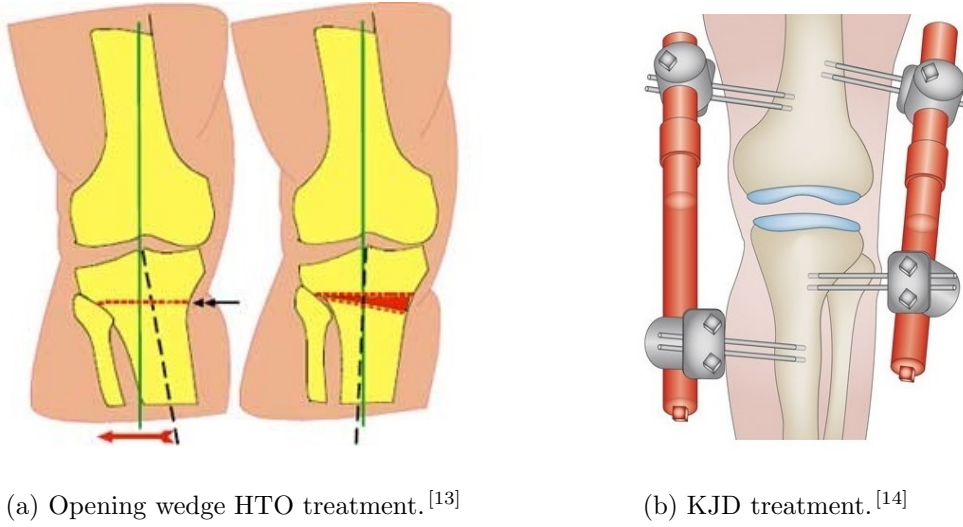


Figure 2: Two possible treatments for OA.

1.3 Study goal

In OA, periarticular bone density is increased due to sclerosis. However, formation of cysts causes decreased densities at certain locations. Previous research showed a normalization of the subchondral bone after distraction of the ankle joint. The mean subchondral bone density was decreased, while abnormally low densities due to cysts increased to more normal densities.^[12] KJD also seems to have good results, but there has never been a qualitative assessment of bone tissue after KJD. Therefore, the main goal of this study is to determine the quality of the periarticular bone by composing 3D images of the knee joint using Computed Tomography (CT). In this research, the quality of periarticular bone was assessed by the bone density of subchondral bone and trabecular bone for both treatments. The main question of this research is: What is the difference in quality of the periarticular bone before and two years after treatment with KJD or HTO, determined by 3D-CT?

2 Methodology

2.1 Computed Tomography

For this research, CT images were used to compose a 3D reconstruction of the tibia, so the intensity displayed by the voxels represent the bone density at a specific anatomical position. The use of CT is an advantage over the conventional bone density measurements, so called DEXA scans, because it assesses the volumetric density (mg/cm^3) rather than the 2D area density (g/cm^2) generated from a DEXA scan.^[15]

Because the DEXA scan is only two dimensional, it calculates the mean intensity along the direction of the scan axis. For this reason, a DEXA scan would be insufficient to assess changes in bone density because the increased and decreased intensities at different locations that can be found in OA will give a mean value that is comparable to the mean intensity in healthy bone tissue. Therefore, the displayed values by use of a DEXA scan are not truly representative for the bone density. The 3D CT reconstruction can display the intensity for every different voxel in the 3D space, making it more suitable to assess changes in bone density.^[16]

2.2 Subjects

Subjects were selected from two trials reviewed by the Medical Ethical Committee (MEC #11-072 and MEC #10-359). Patients were all diagnosed with severe OA of the knee and indicated for a HTO by an orthopaedic surgeon. The inclusion criteria for both trials were set as followed:^[17]

- Patients with medial or lateral tibio-femoral compartmental OA considered for HTO according to regular clinical practice;
- Age < 65 years;
- Radiological joint damage: Kellgren and Lawrence score > 2;
- Intact knee ligaments;
- Normal range-of-motion (min. of 120° flexion);
- Normal stability;
- Body Mass Index < 35.

Exclusion criteria for this research were:

- Mechanic axis-deviation (varus-valgus) < 10 degrees;
- Psychological inabilities or difficult to instruct;
- Not able to undergo MRI examination (standard daily clinical practice protocol);
- Inflammatory or rheumatoid arthritis present or in history;
- Post traumatic fibrosis due to fracture of the tibial plateau;
- Bone-to-bone contact in the joint (absence of any joint space on X-ray);
- Surgical treatment of the involved knee < 6 months ago;
- Contra-lateral knee OA that needs treatment;
- Primary patello-femoral OA.

2.3 Data Collection

CT images of the subjects were provided by the department of Rheumatology and Clinical Immunology, University Medical Center Utrecht, and made by a Phillips Brilliance '64 CT scanner. These CT images were taken prior to treatment (baseline) and at two years of follow up and were obtained in the period from July 2012 to September 2015. To process the data, as described in the following section, scans containing a coronal view of the knee joint were used. Therefore, CT data of 23 patients (mean age 51 ± 7 years; 15 males, 10 KJD) were included.

2.4 Data Processing

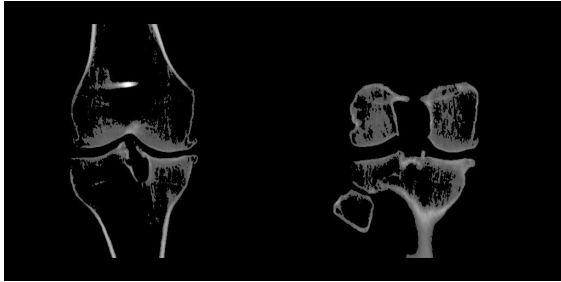
In order to obtain 3D results that can be analysed to assess the quality of the periarticular bone, the data was processed through the actions written below. All processing was done with the use of Matlab R2015b. An overview of the processing steps can be found in a flowchart in appendix I. An explanatory list of certain Matlab commands can be found in appendix II.

2.4.1 Load DICOM files

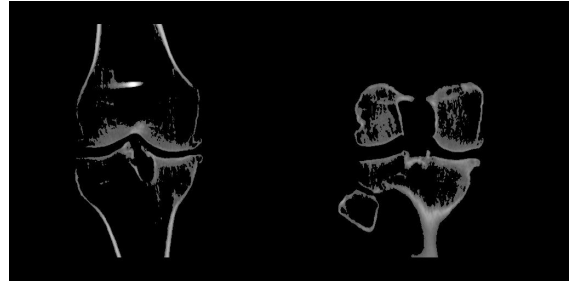
The script that was used to read the DICOM files in Matlab was based on a script retrieved from Matlab Central/File Exchange.^[18] Some adjustments were made to meet specific requirements. The output of the script is a volume image matrix of the loaded DICOM files.

2.4.2 Segmentation

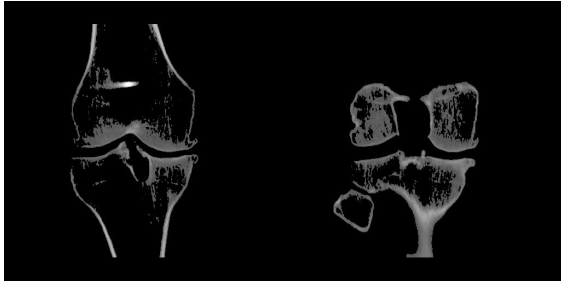
Medical image segmentation is an important part of the data processing. Using segmentation, a region of interest, in this case bone tissue, can be extracted from surrounding tissues in medical images. Many segmentation methods exist, both automatic and semi-automatic.



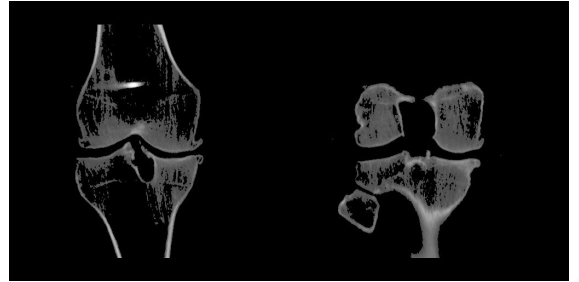
(a) Segmentation based on a global threshold of 306 Hounsfield Units.



(b) Segmentation based on a local threshold obtained with the *imrect* function in Matlab.



(c) Segmentation based on a global threshold obtained with Otsu's method.



(d) Segmentation based on a global threshold by visual assessment.

Figure 3: Different segmentation methods that were considered to segment bone from surrounding tissue.

To extract bone from the surrounding tissue, techniques like global, local and Otsu's thresholding and region growing were considered. A comparison of different segmentation methods, as can be seen in figure 3, showed minimal differences in accuracy. Global thresholding by use of one certain threshold value appeared to be the fastest and least subjective method to segment the bone tissue from the surrounding soft tissue. Therefore, segmentation was done based on one threshold value of 306 Hounsfield Units (HU). This value can separate high intensity voxels (e.g. cortical bone) from low intensity voxels (e.g. soft tissue).^[19]

2.4.3 Splitting tibia and femur

In order to look at the tibial plateau, the femur had to be removed from the 3D reconstruction. Based on the assumption that both tibia and the femur are two different connected structures, the tibia and femur were labelled by the function *bwconncomp* after segmentation. After the labelling of both bones, the femur was removed from the 3D image, based on the height. In order for this method to work the tibial and femur bone cannot be connected at any location in the scan. By using the function *imerode*, all the edges of both bones were reduced by one pixel to minimize the chance that the tibia and femur would still be connected. This created small gaps in the images which were partially repaired using the *imclose* function. Scans that had the tibia and femur still connected after this adjustment were excluded from this research, which was the case in the scans of eight subjects. Apart from splitting the bones, this section of the script was also used to filter the scan. Smaller groups of pixels that were not connected to either the tibia or femur were extracted from the data.

2.4.4 Intensity and location of tibial plateau

Bone changes were tracked by five layers of each 1 mm following the bone contours, to a total depth of 5 mm from the joint surface as shown in figure 4. Layers three up to and including five represent trabecular bone, while layers one and two can contain subchondral bone as well as trabecular bone, depending on anatomical variations. To calculate the number of pixels that was needed to create layers that represented 1 mm the pixelspacing was extracted from the DICOM-info.

To create matrices for different depths in the segmented and splitted tibia that includes data of location and intensity of the tibial plateau, a script was written to extract these values. These matrices were used for visual as well as statistical analysis. The intensity value of each layer was determined by taking the mean of the intensities of the number of pixels that form 1 mm.

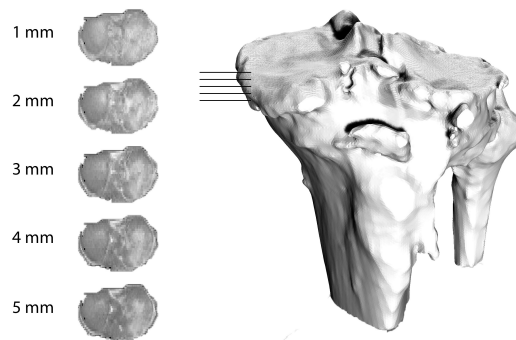


Figure 4: Grayscale images of the tibial plateau at different depths from the surface.

2.4.5 Reconstruction

To check the result of the segmentation visually, a script was retrieved from Matlab Central/File Exchange.^[20] This script requires input data of a 3D image volume of the type double, single, (u)int8, (u)int 16 or (u)int32. In this research, an input of the type uint16 was used. The 3D reconstructions were created with Stradwin 5.1.

Because most changes in intensity and surface were expected to be found in the tibial plateau, an intensity based colour map was plotted over a surface based reconstruction. This was done by plotting two different matrices: one which contained information about the surface, and another with information about the intensity. The tibial plateau was reconstructed by plotting the intensity based colour map on top of the matrix with surface information. In this way, an indication of bone density was given at each location. This was solely used to check if the tibial plateau was created correctly. This was the case in all but one patients, which was removed from the research.

2.5 Measurements and Calculations

In order to show changes in quality of bone tissue, three different areas at the tibial plateau were defined based on the amount of weight bearing. The defined areas were: the tibial plateau underneath the medial and lateral condyle of the femur, and all other parts of the tibial plateau, as shown in figure 5. The two condyles were created by forming a matrix which contained the information of the femur location viewed from bottom up. This matrix was reduced to the point where only the medial and lateral condyles remained. Using this matrix, the weight bearing areas of the tibial plateau were selected.

Changes in bone density were analysed by comparing the mean intensity of each compartment at baseline and two year follow up. Besides the mean value, the Mean Absolute Deviation (MAD) was also calculated, because it was expected that there would be an increase as well as a decrease in the bone density which would be unnoticeable using the mean intensity. The MAD represents the dispersion around the mean intensity of the data and can give more information about the different densities that can be found in the bone. In this way, the quality of the bone can be calculated more reliable. The MAD is expected to be decreased after the treatment. The lateral and medial side of the knee joint were considered separately to see the change in MAD at each side of the knee. Since it is assumed there will be an increase in pressure at one side of the knee and a decrease at the other after HTO.

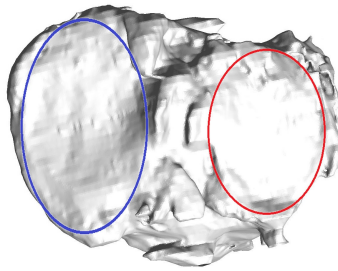


Figure 5: Selection of the medial (blue) and lateral (red) compartments on the tibial plateau was based on the location of the medial and lateral condyle of the femur. The remainder of the tibial plateau is defined as other compartment.

2.6 Statistics

All data was analysed using the statistical analysis software package IBM SPSS Statistics 23. The Shapiro-Wilk Test was used in order to detect if the data showed a normal distribution. For normally distributed data, statistical significance was determined by a paired samples T-test. The variables at baseline and at two year follow-up served as a pair in the samples T-test. When data showed no normal distribution, the nonparametric test Related-Samples Wilcoxon Signed Rank Test was applied. For both paramatric and nonparametric tests, significance level was set at $p = 0.05$.

3 Results

3.1 Mean intensity outcome

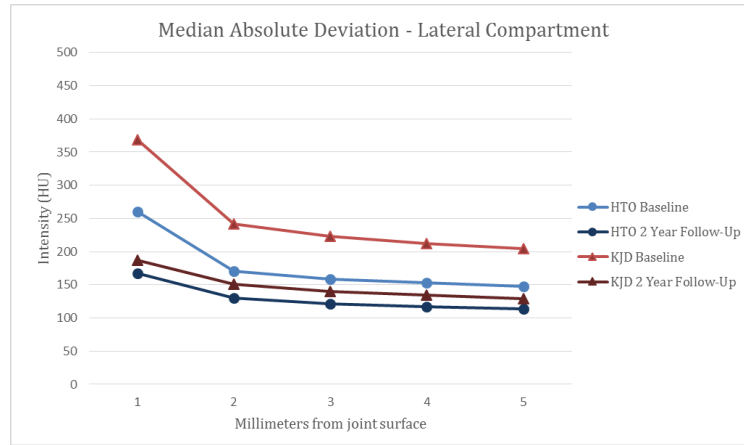
In total, 23 patients could be included to examine bone quality after treatment (13 HTO, 10 KJD). Mean intensities in all three compartments (medial, lateral and other) followed a normal distribution in both KJD and HTO. Although mean intensities at two year follow-up seem to show a decrease relative to baseline, these differences were statistically indistinguishable.

3.2 Mean Absolute Deviation outcome

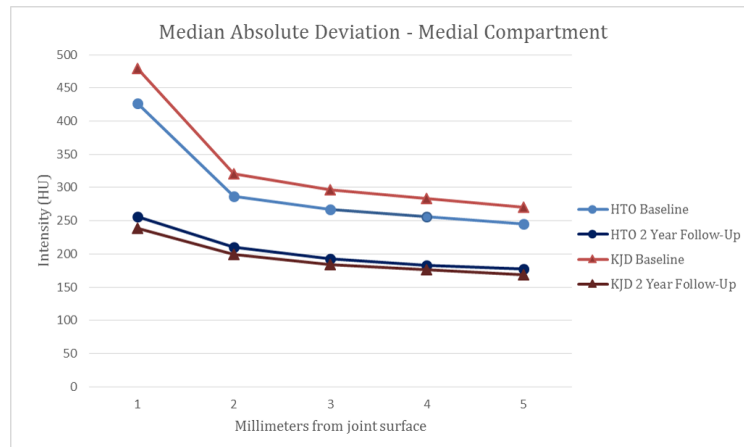
In case of HTO, a nonparametric test showed no significant differences in the MAD in all three compartments. In KJD, not all variables showed a normal distribution in case of MAD so different statistical tests were used. Table 1 shows the results of the parametric and nonparametric tests that were used to determine if KJD had significant change in MAD. Especially in the lateral compartment significant change in MAD can be found.

Compartment	Test used	Significance per millimeter from joint surface
Medial	Related-Samples Wilcoxon Signed Rank Test (nonparametric)	1: $p = 0.028$ (sig.) 2: $p = 0.059$ 3: $p = 0.053$ 4: $p = 0.041$ (sig.) 5: $p = 0.059$
Lateral	Paired-Samples T Test (parametric)	1: $p = 0.029$ (sig.) 2: $p = 0.025$ (sig.) 3: $p = 0.026$ (sig.) 4: $p = 0.027$ (sig.) 5: $p = 0.029$ (sig.)
Other	Related-Samples Wilcoxon Signed Rank Test (nonparametric)	1: $p = 0.047$ (sig.) 2: $p = 0.059$ 3: $p = 0.059$ 4: $p = 0.059$ 5: $p = 0.059$

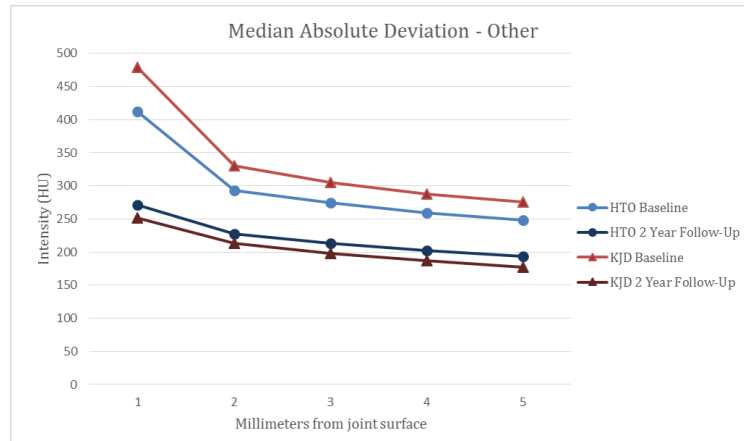
Table 1: Results statistical significance per millimeter from joint surface for KJD treatment. Baseline and two year follow-up were compared.



(a) MAD Graph lateral compartment



(b) MAD Graph medial compartment



(c) MAD Graph surface other than lateral and medial compartments

Figure 6: Graphs of MAD at baseline and two year follow-up after treatment with HTO or KJD.

In figure 6 can be seen that MAD has decreased for both HTO and KJD treatment in all compartments in 1-5 mm from the joint surface. MAD decreased more after KJD in comparison to HTO at baseline and two year follow-up. MAD also decreased with each millimeter in depth. It should be noticed that at baseline MAD at 1 mm from the joint surface was higher than at 2-5 mm for both the HTO and KJD treatment.

After treatment with HTO, changes in bone density were visible in especially the lateral compartment. In figure 7 the lateral compartment shows an increase in intensity, and therefore bone density, at the two year follow-up image. After treatment with KJD a change in intensity was also visible. In figure 8 the medial compartment shows a decrease in intensity.

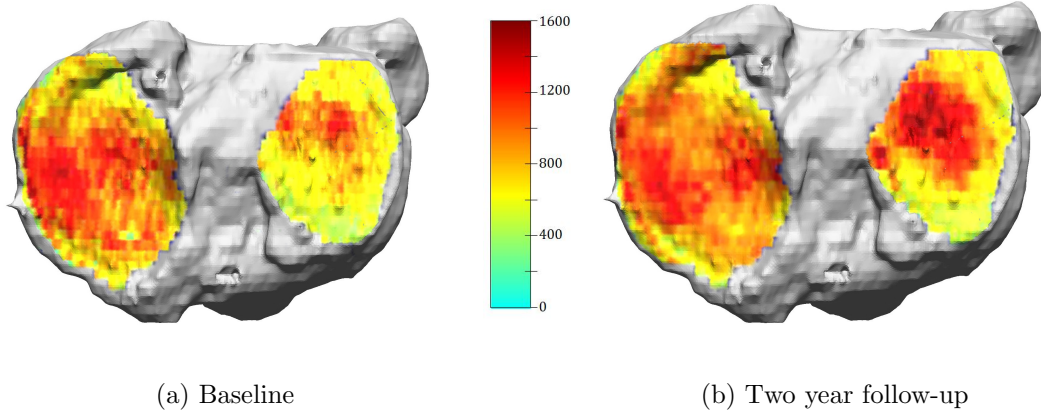


Figure 7: Intensity based colour map of the lateral and medial compartment was reconstructed on tibial plateau. Images of one subject at baseline and two year follow-up after treatment with HTO are shown in HU.

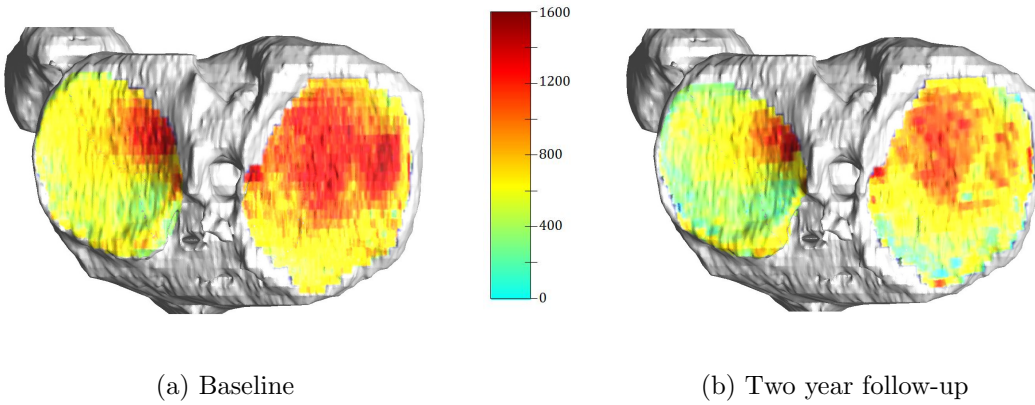


Figure 8: Intensity based colour map of the lateral and medial compartment was reconstructed on tibial plateau. Images of one subject at baseline and two year follow-up after treatment with KJD are shown in HU.

4 Discussion

The aim of this study is to determine what the influence is of KJD and HTO on the quality of the periarticular bone. This was done by assessment of different variables in different depths of the tibial bone that represent bone density. The mean intensity and the MAD were reviewed for the weight bearing areas underneath the medial and lateral condyles of the femur in particular. The results show that there is no statistical significant difference in mean intensity for all the different areas after both HTO and KJD. However, the results show a slight decrease in intensity after both treatments. The fact that there is no significant change in the mean intensity could be explained by cyst formation in OA. The cysts that are formed in bone tissue have low intensity values on CT images. The bone tissue also contains parts with scleroses that have high values on CT images. Because these values neutralize each other in a mean intensity value, the mean intensity at two year follow-up may not be that much different from the mean intensity calculated at baseline. As a result, change in bone density is harder to statistically prove.

To overcome this effect, this research focusses on the MAD because it displays absolute changes in the bone density. The MAD after KJD significantly decreases in the medial, lateral and other compartments of the tibial plateau. This shows that after the treatment the bone density of the periarticular bone of the tibia neutralizes, meaning the quality shifts towards the quality of healthy bone. This indicates that KJD is a suitable method to treat patients suffering from OA. However, the results of the patients treated with HTO do not show significant changes in the MAD. This can be explained by the fact that HTO is a more invasive procedure which results in more damage to the bone. Because the shift in weight bearing areas caused by HTO, which is the main principle of this procedure, quality improvement of the subchondral and trabecular bone does not necessarily have to occur. As a result of this shift in weight bearing, pressure areas also change. In some scans there was an increase in intensity visible in the lateral compartment due to the increased pressure on this side of the tibial plateau. Since patients treated with HTO have a main affected side, the treatment could help in reducing pain, because HTO showed little decrease in bone density on the main affected side.

4.1 Computed Tomography settings

The displayed HU for a certain structure might not be the same for every scan, since the HU scale is normalized to the brightness and contrast of distilled water at standard pressure and temperature. The Hounsfield scale is linear between two points:

$$1000 \times \frac{\mu_{(x,y)} - \mu_{water}}{\mu_{water}} \quad (1)$$

Because the polyenergetic output for each CT scanner is different, but also for the same scanner with different settings, the attenuating properties may vary. This means the x-ray beam spectrum can vary and therefore the number of HU can not be compared directly. To overcome this problem there are two valid solutions, the first one is using dual energy radiography. This is a method using a high and low energy acquisition, this way the energy dependant factors can be mathematically excluded. The other solution is by use of a phantom with known density. In this case, the density of the phantom is known and a HU value will be given, which makes it possible to compare the other structures in the scan to this density.^[21]

Since the CT images were made before the start of this research, the use of a phantom nor dual energy radiography was possible. For the CT images used in this research the same CT scanner was used and all settings were equal except for the Peak KiloVoltage (kVp) for one patient. The kVp was set at 120 kVp for all patients but one, a value of 100 kVp was chosen for this CT scan. for the scans at baseline and at two year follow-up of that patient that were to be compared with unequal settings, the x-ray spectra were found within a similar window as shown in figure 9. Because of the similar x-ray spectrum it was decided to include these CT scans in the research.

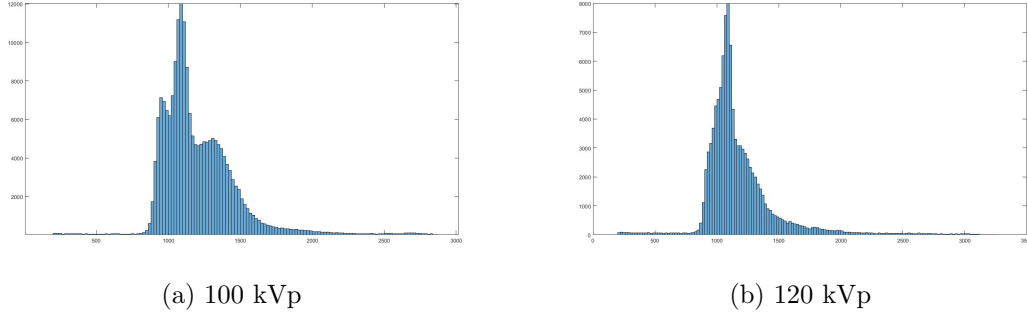


Figure 9: X-Ray spectrum of the CT-images. In both spectra can be seen that the values focus around the same point, indicating that there is no shift in values due to the difference in kVp.

4.2 Future recommendations

4.2.1 Partial volume effect

An aspect that has to be taken into account when using CT data is the partial volume effect. Because voxels have a certain size, different types of tissue can be captured within the same voxel, resulting in a mean voxel intensity of those tissues. This effect could have had a significant influence on the outcome of this research, since it mainly looked at bone surfaces.

For future research, this effect could be reduced to a minimum by selecting scans with the lowest possible slice thickness.

4.2.2 Ultra thin slices

Just after the script was nearly finished, ultra thin slices were available. These ultra thin slices were made in axial view, instead of the coronal view the script was originally written for. Because ultra thin slices consist of more data, they were expected to be more accurate. Also, the partial volume effect would be reduced when using these ultra thin slices. Therefore, this data was loaded into the script after using the *permute* function to reconstruct the coronal slices. As a result, the proportions of the images were incorrect and there was more noise after segmentation than in the original coronal slices. To fix these problems, a large part of the script should be rewritten and keeping the time to the deadline in mind, the choice was made to keep using the original, less thin, coronal slices.

For the future it would be recommended to use ultra thin slices, since it can highly improve the accuracy of the calculations.

4.2.3 Segmentation

Several threshold methods for segmentation were considered, but eventually a value based on literature study was chosen. This was done because the difference in accuracy for the different methods seemed minimal, the results would be less influenced because the threshold value is the same in every scan and the script was much faster this way. Nevertheless, a more advanced threshold method could improve the segmentation of the bone tissue, especially because the written script is not capable of splitting the bones when the segmented tibia and femur were connected with several voxels. During the research this led to the exclusion of eight subjects. Since the excluded subjects were of both the KJD and HTO groups, it is assumed that the exclusion did not affect the outcome of this research. For future researches, it is recommended to include a larger population which would increase the validity of the study.

Also, when looking at the results this threshold method seems not fully capable of filtering all soft tissue. The first layer, surface until 1 mm depth, had a very large range of intensity values, which is not expected in bone tissue. When zooming in at the image of this layer, a small layer of one pixel of surrounding soft tissue could be seen. This layer was filtered away with an *erode* function in Matlab, but in some cases the segmentation and the erode function created gaps in the tibial bone. Smaller gaps could be closed by using the function *imclose* in Matlab but this was insufficient for larger gaps. This resulted in a loss of data that could have influenced the outcome of this research. In this research the limited time resulted in imperfect segmented bone.

Since the segmentation of the tibial bone plays such a crucial role in the reconstruction of the tibial plateau, it is essential that this process works as good as possible. For future research the segmented bone should be optimized before continuing the calculations. When the bone contains less gaps and noise the measurements will be more reliable and significant changes will be easier to prove. Perhaps different segmentation methods should be considered apart from thresholding. Altogether, a more advanced segmentation method could improve the segmentation step and therefore all following steps in the script.

4.3 Conclusion

The results of this research indicate that periarticular bone density changes in response to KJD and HTO. The mean densities showed a slight decrease after two years but could not be significantly proven for either procedure. The changes of MAD in patients treated with HTO were also statistically indistinguishable. However, the MAD did significantly change with patients undergoing KJD. This suggests that periarticular bone density neutralizes and that joint distraction has a positive effect on the quality of the bone.

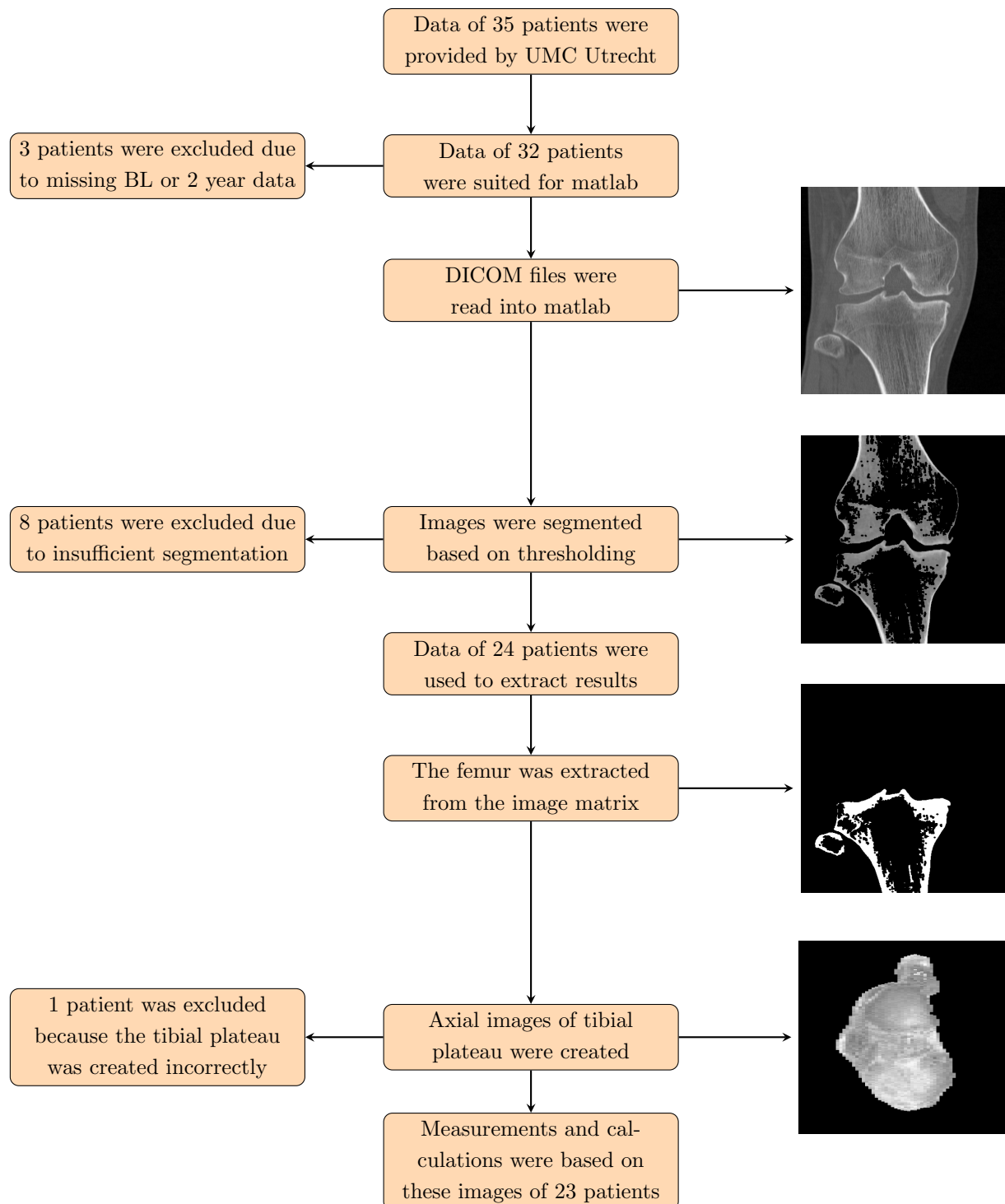
References

- [1] Wittenauer R. Smith L. Aden K. Tanna, S. Update on 2004 background paper 6.12 osteoarthritis. http://www.who.int/medicines/areas/priority_medicines/BP6.12Osteo.pdf, January 2013. Accessed: May 9, 2016.
- [2] Gommer A. Poos M. Hoe vaak komt artrose voor en hoeveel mensen sterven eraan? <http://www.nationaalkompas.nl/gezondheid-en-ziekte/ziekten-en-aandoeningen/bewegingsstelsel-en-bindweefsel/artrose/omvang/>, June 2014. Accessed: April 19, 2016.
- [3] James A Martin and Joseph A Buckwalter. Roles of articular cartilage aging and chondrocyte senescence in the pathogenesis of osteoarthritis. *Iowa Orthopaedic Journal*, 21:1–7, 2001.
- [4] Linda Troeberg and Hideaki Nagase. Proteases involved in cartilage matrix degradation in osteoarthritis. *Biochimica et Biophysica Acta (BBA)-Proteins and Proteomics*, 1824(1):133–145, 2012.
- [5] DT Felson, DR Gale, M Elon Gale, J Niu, DJ Hunter, J Goggins, and MP Lavalley. Osteophytes and progression of knee osteoarthritis. *Rheumatology*, 44(1):100–104, 2005.
- [6] S Milz and Reinhard Putz. Quantitative morphology of the subchondral plate of the tibial plateau. *Journal of anatomy*, 185(Pt 1):103, 1994.
- [7] Anne Ballinger. *Essentials of Kumar and Clark's Clinical Medicine*. Elsevier Health Sciences, 2011.
- [8] KM Jordan, NK Arden, Michael Doherty, Bernard Bannwarth, JWW Bijlsma, Paul Dieppe, K Gunther, Hans Hauselmann, Gabriel Herrero-Beaumont, Phaedon Kaklamanis, et al. Eular recommendations 2003: an evidence based approach to the management of knee osteoarthritis: Report of a task force of the standing committee for international clinical studies including therapeutic trials (escisit). *Annals of the rheumatic diseases*, 62(12):1145–1155, 2003.
- [9] Dong Chul Lee and Seong Joon Byun. High tibial osteotomy. *Knee surgery & related research*, 24(2):61–69, 2012.
- [10] Karen Wiegant. Knee joint distraction. intrinsic cartilage repair and sustained clinical benefit. 2015.
- [11] JJW Ploegmakers, PM Van Roermund, J Van Melkebeek, Johan Lammens, JWW Bijlsma, FPJG Lafeber, and ACA Marijnissen. Prolonged clinical benefit from joint distraction in the treatment of ankle osteoarthritis. *Osteoarthritis and cartilage*, 13(7):582–588, 2005.
- [12] F Intema, TP Thomas, DD Anderson, JM Elkins, TD Brown, A Amendola, FPJG Lafeber, and CL Saltzman. Subchondral bone remodeling is related to clinical improvement after joint distraction in the treatment of ankle osteoarthritis. *Osteoarthritis and Cartilage*, 19(6):668–675, 2011.
- [13] A Cazenave. High valgus tibial osteotomy. <http://www.orthopale.com/tibial-osteotomy.php>, 12 2007.
- [14] Simon C Mastbergen, Daniël BF Saris, and Floris PJG Lafeber. Functional articular cartilage repair: here, near, or is the best approach not yet clear? *Nature reviews rheumatology*, 9(5):277–290, 2013.
- [15] Joseph J Schreiber, Paul A Anderson, and Wellington K Hsu. Use of computed tomography for assessing bone mineral density. *Neurosurgical focus*, 37(1):E4, 2014.
- [16] Judith E Adams. Quantitative computed tomography. *European journal of radiology*, 71(3):415–424, 2009.
- [17] F P J G Lafeber and K Wiegant. Trial info: Knee joint distraction in comparison with high tibial osteotomy in treatment of knee osteoarthritis. <http://www.trialregister.nl/trialreg/admin/rctview.asp?TC=2900>, may 2011.

- [18] A. Balter. Dicom23d, in: 3d visualization of density distribution. http://nl.mathworks.com/matlabcentral/fileexchange/45949-3d-visualization-of-density-distribution?s_tid=srchtitle, 2009. Pacific Northwest National Laboratory. Accessed: May 10 2016.
- [19] Abdal M Alyassin and Gopal B Avinash. Semiautomatic bone removal technique from ct angiography data. In *Medical Imaging 2001*, pages 1273–1283. International Society for Optics and Photonics, 2001.
- [20] D.J. Kroon. Viewer3d, in: Medical viewer. <http://www.mathworks.com/matlabcentral/fileexchange/21993-viewer3d>, 11 2008.
- [21] Alex AT Bui and Ricky K Taira. *Medical imaging informatics*. Springer Science & Business Media, 2009.

Appendices

Appendix I Flowchart Methodology



Appendix II List of Matlab Commands

Bwconncomp: finds the connecting pixels in 3D space. A value of connectivity can be specified.

Imclose: closes gaps in an image with a specified shape and size.

Imerode: removes specified number of pixels from the boundaries of connected pixels.

Imrect: creates an interactive tool in which the user can select a certain rectangle area using the mouse. Different values can be extracted from the selected area, for example position of the edges and values of the pixels within the rectangle.

Permute: rearranges dimensions of 3D matrix.

Appendix III Matlab Script

```
1 %% read dicom files
2
3 for g = 1:2
4 clearvars -except g;
5 close all;
6
7 default_dicom_fields = {...
8     'Filename',...
9     'Height', ...
10    'Width', ...
11    'Rows',...
12    'Columns', ...
13    'PixelSpacing',...
14    'SliceThickness',...
15    'SliceLocation',...
16    'ImagePositionPatient',...
17    'ImageOrientationPatient',...
18    'FrameOfReferenceUID',...
19 };
20
21 % We need these checks because to calculate the "extra_fields", we
22 % need to have the PixelSpacing and SliceThickness data. If not, we
23 % leave out the extra_fields.
24 no_pixel_spacing = false;
25 no_slice_thickness = false;
26
27 extra_fields = {...
28     'PhysicalHeight',... % Height (cols) of slice in mm
29     'PhysicalWidth',... % Width (rows) of slice in mm
30     'PixelSliceLocation',... % Slice z-location in pixels
31     'PixelSliceThickness',... % Slice thickness in pixels
32     'SliceData'... % The slice image data
33 };
34
35
36 dicom_directory = uigetdir();
37 all_fields = [default_dicom_fields, extra_fields];
38
39 % Get directory listing
40 listing = dir(dicom_directory);
41 % number of files
42 N = numel(listing); % How many entries in the directory listing
43 if (N<3)
44     error('Empty folder');
45     return
46 end
47
48 slice_data(N) = cell2struct(cell(size(all_fields)), all_fields, 2);
49
50 h = waitbar(0,'Reading DICOM Files...','WindowStyle','modal');
```

```

51
52 true_index = 0; % a sequential index of dicom files, that is ignoring
53 % files of other types.
54
55 for i = 3:length(listing) % loop through directory listing, but skip '.' and '..'
56     filename = listing(i).name;
57     [dummy_path, just_the_name, extension] = fileparts(filename);
58     full_path = fullfile(dicom_directory, filename);
59
60     goodfile = false;
61
62     % Check for good dicom file
63     if isdicom(full_path)
64         true_index = true_index + 1;
65         header = dicominfo(full_path);
66         slice_image = dicomread(header);
67
68         % Save selected header data into the structure slice_data
69         for j = 1:numel(default_dicom_fields) % loop through dicom field names
70             current_field = default_dicom_fields{j};
71             % Deal with requested fields not found in header
72             if isfield(header, current_field)
73                 slice_data(true_index).(current_field) = header.(current_field);
74             else
75                 ['header did not contain the field ' current_field]
76             end %if
77
78         end % loop through dicom field names
79         % done saving filtered header data
80
81         % Save slice data
82         slice_data(true_index).SliceData = slice_image;
83         % Save extra fields
84         needed_header_tags = [...
85             isfield(header, 'PixelSpacing'), ...
86             isfield(header, 'SliceThickness'), ...
87             isfield(header, 'SliceLocation')...
88         ];
89
90         if all(needed_header_tags)
91             pixel_spacing = header.PixelSpacing;
92             slice_data(true_index).PhysicalHeight = ...
93                 double(pixel_spacing(1)*header.Columns);
94             slice_data(true_index).PhysicalWidth = ...
95                 double(pixel_spacing(2)*header.Rows);
96             % need to double check which aspect ratio goes with cols/rows
97             slice_data(true_index).PixelSliceLocation = ...
98                 header.SliceLocation / mean(pixel_spacing);
99             slice_data(true_index).PixelSliceThickness = ...
100                 header.SliceThickness / mean(pixel_spacing);
101         else
102             no_pixel_spacing = true;
103         end % if pixel spacing
104

```

```

105     end % if isdicom
106
107     waitbar(i/N,h);
108 end % loop through directory listing
109 % Eliminate empty structs at end.
110 slice_data = slice_data(1:true_index);
111
112 waitbar(1,h);
113 close(h);
114 warning on;
115
116 % Check that some dicom slice was found
117 if true_index < 1
118     'No dicom slices found...returning empty'
119     volume_image = [];
120     slice_data = [];
121     image_meta_data = [];
122     return
123 end
124
125 % If SliceLocation is known, sort by that. This is deemed more
126 % accurate than going by filename order (or file number).
127 if isfield(slice_data(1), 'SliceLocation')
128     [S,I] = sort([slice_data.SliceLocation]);
129     slice_data = slice_data(I);
130 end
131
132 pixelspacing = round(slice_data(true_index).PixelSliceThickness);
133 % Pre-allocate volume image array
134 [rows, cols] = size(slice_data(1).SliceData);
135 volume_image = ...
136     zeros(rows, cols, (length(slice_data)*pixelspacing));
137
138 % Build volume image array
139 h = waitbar(0,'Writing slice images to volume image array...','WindowStyle','modal');
140 for i = 1:length(slice_data)
141     waitbar(i/N,h);
142     volume_image(:, :, (i*pixelspacing)) = slice_data(i).SliceData;
143     for j = 1:pixelspacing-1
144         volume_image(:, :, (i*pixelspacing)-j) = slice_data(i).SliceData;
145     end
146 end
147 close(h);
148 a = size(volume_image);
149 num_slices = a(3);
150
151 %% Threshold 3d-volume based on value from literature
152 middleslice = round(num_slices/2);
153 HU = 306;% Thresholdvalue in HU
154 Threshold = HU + 1024;% Thresholdvalue in grayscale. 1024 is from the dicominfo
155 T = volume_image > Threshold;
156 VI.T1 = volume_image .* T;
157 Threshold2 = Threshold;
158 %% filling and smoothing bone surface

```



```

159     se = strel('disk',1);
160     SE = strel('line',3,0);
161     for i = 1:num_slices
162         test = VI_T1(:, :, i);
163         test = imclose(test, SE);
164         IR = imerode(test, se);
165         VI_T(:, :, i) = IR;
166     end
167     %% Filtering & Splitting based on position of labels
168     figure(1), imshow(VI_T(:, :, middleslice), [])
169     title('Click inbetween tibia and femur')
170     [xtb, ytb, tbvalue] = impixel
171     close(1)
172
173     Label = bwconncomp(VI_T, 18);
174     numlabels = max(size(Label.PixelIdxList));
175     L = zeros([rows, cols, num_slices]);
176     n = 1;
177
178     for i = 1:numlabels
179         freq = max(size(Label.PixelIdxList{1, i}));
180         if freq > 10000
181             for j = 1:freq
182                 p = Label.PixelIdxList{1, i}(j);
183                 L(p) = n;
184             end
185             n = n + 1;
186         end
187     end
188
189     numlabels = max(L(:));
190     FFL = L;
191     for i = 1:numlabels
192         [Y1, X1] = find(L==i); % finding coordinates of areas
193         MY1 = mean(Y1); % mean Y coordinate
194         if MY1 < (ytb) % deleting areas below mean frequency
195             L(L==i) = 0;
196         end
197     end
198     % finding and deleting unwanted stuff
199     figure(1), imshow(L(:, :, middleslice))
200     title('Finding and deleting unwanted stuff, if none: click black')
201     pixel_values = impixel;
202     size_pixel_values = size(pixel_values);
203     close(1)
204     if pixel_values(1, 1) ~= 0
205         for i = 1:size_pixel_values(1)
206             P = pixel_values(i, 1);
207             L(L==P) = 0;
208         end
209     end
210     L = logical(L);
211     result = VI_T .* L;
212

```

```

213 %% creating femur location
214 figure(1),imshow(FFL(:, :,middleslice))
215 title('Click femur')
216 pixel_values = impixel;
217 pixel_values = mean(pixel_values);
218 close(1)
219 h = waitbar(0,'Creating femur location','WindowStyle','modal');
220 FL = zeros([10,10]);
221 for i = 1:num.slices
222     for j = 1:512
223         for k = 200:512
224             if FFL(513-k,j,i) == pixel_values
225                 FL(j,i) = 513-k;
226                 break
227             else
228                 FL(j,i) = 0;
229             end
230         end
231     end
232     waitbar(i/num.slices,h)
233 end
234 FL(FL==0) = NaN;
235 close(h);
236 %% finding place where condyles are parted
237 FL1 = uint16(FL);
238 b = bwlabel(FL1);
239 for i = 1:1000
240     flmin = min(FL1(FL1>0));
241     FL1(FL1==flmin) = 0;
242     b = bwlabel(FL1);
243     if max(b(:)) > 1
244         for j = 1:max(b(:))
245             if max(size(find(b==j))) < 100
246                 [x,y] = find(b==j);
247                 b(b==j) = 0;
248                 FL1(x,y) = 0;
249             end
250         end
251     b = bwlabel(b);
252 end
253 if max(b(:)) > 1
254     figure(1),imshow(b,[])
255     bweg = impixel;
256     bweg = mean(bweg);
257     if bweg == 0
258         close(1)
259         cut_off = min(FL1(FL1>0));
260         flmin = min(FL1(FL1>0));
261         FL1(FL1==flmin) = 0;
262         flmin = min(FL1(FL1>0));
263         FL1(FL1==flmin) = 0;
264         break
265     else
266         [x,y] = find(b==bweg);

```

```

267         for k = 1:max(size(x))
268             FL1(x(k),y(k)) = 0;
269         end
270     end
271 end
272 end
273 condyles = logical(FL1);
274 condyles = imfill(condyles, 'holes');
275 %% crop image based on cut off value
276 [X,Y] = find(L==1);
277 cut_off = cut_off - 15;
278 result_cropped = result(cut_off:end, :, :);
279 VI_cropped = volume_image(cut_off:end, :, :);
280
281 %% creating tibia plateaus for different layers.
282 info = dicominfo(full_path);
283 difY = (512-cut_off);
284 difX = 512;
285 num_pixels = 10;
286 pixpermm = round((slice_data(true_index).PixelSliceThickness)/
287     (slice_data(true_index).SliceThickness));
288 h = waitbar(0, 'Creating tibial plateau grayscale-map', 'WindowStyle', 'modal');
289
290 for i = 1:num_slices
291     for j = 1:(difX)
292         for k = 1:(difY-(5*pixpermm))
293             if result_cropped(k,j,i) ~= 0
294                 for l = 1:pixpermm
295                     pixels1(l) = VI_cropped((k+(l-1)), j, i);
296                     pixels2(l) = VI_cropped((k+(l-1)+pixpermm), j, i);
297                     pixels3(l) = VI_cropped((k+(l-1)+(2*pixpermm)), j, i);
298                     pixels4(l) = VI_cropped((k+(l-1)+(3*pixpermm)), j, i);
299                     pixels5(l) = VI_cropped((k+(l-1)+(4*pixpermm)), j, i);
300                 end
301                 t_plat_gray(j,i,1) = mean(pixels1);
302                 t_plat_gray(j,i,2) = mean(pixels2);
303                 t_plat_gray(j,i,3) = mean(pixels3);
304                 t_plat_gray(j,i,4) = mean(pixels4);
305                 t_plat_gray(j,i,5) = mean(pixels5);
306                 t_plat_loc(j,i) = k;
307                 break
308             else
309                 t_plat_gray(j,i,:) = NaN;
310                 t_plat_loc(j,i) = NaN;
311             end
312         end
313     end
314     waitbar(i/num_slices, h)
315 end
316 close(h)
317 H1=t_plat_gray(:, :, 1); H2=t_plat_gray(:, :, 2); H3=t_plat_gray(:, :, 3); H4=t_plat_gray(:, :, 4);
318     H5=t_plat_gray(:, :, 5);
319 montage1 = [H1 H2 H3 H4 H5];
320 imshow(montage1, [])

```

```

321 %% deleting holes from tibia plateau location
322 TPL = 512 - t_plat_loc;
323
324 depth = 10;
325 cut_off1 = mode(TPL(:))-(depth*pixpermm);
326 TPL(TPL<cut_off1) = 0;
327 imshow(TPL,[])
328 %creating logical of tibia plateau
329 TPL(isnan(TPL))=0;
330 TPlogical = bwlabel(TPL,8);
331 num_labels = max(TPlogical(:));
332 for i = 1:num_labels
333     freq(i) = max(size(find(TPlogical(TPlogical==i))));
334 end
335 maxfreq = find(freq==max(freq(:)));
336 TPlogical(TPlogical~=maxfreq) = 0;
337 TPlogical = logical(TPlogical);
338 %creating logical of condyles(lateral and medial)
339 TPG = t_plat_gray(:,:,1);
340 num_layers = 5;
341 b = bwlabel(condyles);
342 figure(1)
343 imshow(TPG,[])
344 figure(2)
345 imshow(b)
346 title('Select lateral condyle')
347 pixlatcon = impixel;
348 close([1 2])
349 pixlatcon = pixlatcon(1,1);
350 bm = b;
351 bm(bm==pixlatcon) = 0;
352 bm = logical(bm);
353 bl = b;
354 bl(bl~=pixlatcon) = 0;
355 bl = logical(bl);
356 rest = ~condyles;
357 rest = logical(rest);
358 %%
359 for i = 1:5
360     TPG = t_plat_gray(:,:,i);
361     TPG = TPG.*TPlogical;
362     plateaus(:,:,i) = TPG;
363 end
364
365 %% Save data
366 fileloc = char(dicom_directory);
367 filename = [ fileloc '.mat' ];
368 save(filename,'num_slices',...
369     'volume_image',...
370     'info',...
371     'result_cropped',...
372     'TPL',...
373     'condyles',...
374     'plateaus',...

```

```

375     'bm',...
376     'bl',...
377     'rest'...
378 );
379
380 end

1  % open saved data
2  clear all
3
4  voor = load(['VOOR.mat']);
5  na = load(['NA.mat']);
6  %% selecting which condyles you want to use
7  montage = [voor.condyles na.condyles];
8  figure(1)
9  imshow(montage, [])
10 title('Voor Na')
11 prompt = 'Which condyles do you want to use?? ';
12 str = input(prompt, 's');
13 close(1)
14
15 if strcmp(str, 'voor') == 1
16     welke_is_wat = 'voor is fixed';
17     condyles = voor.condyles;
18     bm = voor.bm;
19     bl = voor.bl;
20     rest = voor.rest;
21     Fixed = voor.plateaus;
22     Moving = na.plateaus;
23 else
24     welke_is_wat = 'na is fixed';
25     condyles = na.condyles;
26     bm = na.bm;
27     bl = na.bl;
28     rest = na.rest;
29     Fixed = na.plateaus;
30     Moving = voor.plateaus;
31 end
32 %% imregister before and after
33 for k = 1:5
34     fixed = uint16(Fixed(:, :, k));
35     moving = uint16(Moving(:, :, k));
36
37     [optimizer, metric] = imregconfig('monomodal');
38     MR(:, :, k) = imregister(moving, fixed, 'affine', optimizer, metric);
39 end
40 %% calculating different values for fixed
41 for i = 1:5
42     TPG = Fixed(:, :, i);
43
44     A = TPG;
45     TPGM = A.*bm;
46     TPGL = A.*bl;

```

```

47 Rest = A.*rest;
48 TPGC = A.*condyles;
49
50 meantotal = round(mean(A(A>0)));
51 modustotal = mode(A(A>0));
52 MADtotal = round(nanmean(mad(A)));
53 skewtotal = skewness(A(:));
54 kurttotal = kurtosis(A(:));
55
56 meanmedial = round(mean(TPGM(TPGM>0)));
57 modusmedial = mode(TPGM(TPGM>0));
58 MADmedial = round(nanmean(mad(TPGM)));
59 skewmedial = skewness(TPGM(:));
60 kurtmedial = kurtosis(TPGM(:));
61
62 meanlateral = round(mean(TPGL(TPGL>0)));
63 moduslateral = mode(TPGL(TPGL>0));
64 MADlateral = round(nanmean(mad(TPGL)));
65 skewlateral = skewness(TPGL(:));
66 kurtlateral = kurtosis(TPGL(:));
67
68 meanrest = round(mean(Rest(Rest>0)));
69 modusrest = mode(Rest(Rest>0));
70 MADrest = round(nanmean(mad(Rest)));
71 skewrest = skewness(Rest(:));
72 kurtrest = kurtosis(Rest(:));
73
74 meancondyles = round(mean(TPGC(TPGC>0)));
75 moduscondyles = mode(TPGC(TPGC>0));
76 MADcondyles = round(nanmean(mad(TPGC)));
77 skewcondyles = skewness(TPGC(:));
78 kurtcondyles = kurtosis(TPGC(:));
79
80 mean_values.fixed(i) = struct('meantotal',meantotal,'modustotal',modustotal,'MADtotal',MADtotal,
81     'skewtotal',skewtotal,'kurttotal',kurttotal,...
82     'meanmedial',meanmedial,'modusmedial',modusmedial,'MADmedial',MADmedial,'skewmedial',
83     skewmedial,'kurtmedial',kurtmedial,...
84     'meanlateral',meanlateral,'moduslateral',moduslateral,'MADlateral',MADlateral,'skewlateral',
85     skewlateral,'kurtlateral',kurtlateral,...
86     'meancondyles',meancondyles,'moduscondyles',moduscondyles,'MADcondyles',MADcondyles,
87     'skewcondyles',skewcondyles,'kurtcondyles',kurtcondyles,...
88     'meanrest',meanrest,'modusrest',modusrest,'MADrest',MADrest,'skewrest',skewrest,'kurtrest',
89     kurtrest);
90 end
91 %% calculating different values for movingregistered
92 MR = double(MR);
93 for i = 1:5
94     TPG = MR(:, :, i);
95
96 A = TPG;
97 TPGM = A.*bm;
98 TPGL = A.*bl;
99 Rest = A.*rest;
100 TPGC = A.*condyles;

```

```

101
102 meantotal = round(mean(A(A>0)));
103 modustotal = mode(A(A>0));
104 MADtotal = round(nanmean(mad(A)));
105 skewtotal = skewness(A(:));
106 kurttotal = kurtosis(A(:));
107
108 meanmedial = round(mean(TPGM(TPGM>0)));
109 modusmedial = mode(TPGM(TPGM>0));
110 MADmedial = round(nanmean(mad(TPGM)));
111 skewmedial = skewness(TPGM(:));
112 kurtmedial = kurtosis(TPGM(:));
113
114 meanlateral = round(mean(TPGL(TPGL>0)));
115 moduslateral = mode(TPGL(TPGL>0));
116 MADlateral = round(nanmean(mad(TPGL)));
117 skewlateral = skewness(TPGL(:));
118 kurtlateral = kurtosis(TPGL(:));
119
120 meanrest = round(mean(Rest(Rest>0)));
121 modusrest = mode(Rest(Rest>0));
122 MADrest = round(nanmean(mad(Rest)));
123 skewrest = skewness(Rest(:));
124 kurtrest = kurtosis(Rest(:));
125
126 meancondyles = round(mean(TPGC(TPGC>0)));
127 moduscondyles = mode(TPGC(TPGC>0));
128 MADcondyles = round(nanmean(mad(TPGC)));
129 skewcondyles = skewness(TPGC(:));
130 kurtcondyles = kurtosis(TPGC(:));
131 %save calculated data to struct
132 mean_values_MR(i) = struct('meantotal',meantotal,'modustotal',modustotal,'MADtotal',MADtotal,
133     'skewtotal',skewtotal,'kurttotal',kurttotal,...
134     'meanmedial',meanmedial,'modusmedial',modusmedial,'MADmedial',MADmedial,'skewmedial',
135     skewmedial,'kurtmedial',kurtmedial,...
136     'meanlateral',meanlateral,'moduslateral',moduslateral,'MADlateral',MADlateral,'skewlateral',
137     skewlateral,'kurtlateral',kurtlateral,...
138     'meancondyles',meancondyles,'moduscondyles',moduscondyles,'MADcondyles',MADcondyles,
139     'skewcondyles',skewcondyles,'kurtcondyles',kurtcondyles,...
140     'meanrest',meanrest,'modusrest',modusrest,'MADrest',MADrest,'skewrest',skewrest,'kurtrest',
141     kurtrest);
142 end
143 %% renaming fixed and MR
144 if strcmp(str,'voor') == 1
145     MVvoor = mean_values_fixed;
146     MVna = mean_values_MR;
147 else
148     MVvoor = mean_values_MR;
149     MVna = mean_values_fixed;
150 end
151 %%
152 MR = double(MR);
153 for i = 1:5
154     for j = 1:size(Fixed,1)

```

```

155     for k = 1:size(Fixed,2)
156         if Fixed(j,k,i) == 0
157             diff(j,k,i) = 0;
158         elseif MR(j,k,i) == 0
159             diff(j,k,i) = 0;
160         else
161             if strcmp(str,'voor') == 1
162                 diff(j,k,i) = abs(Fixed(j,k,i) - MR(j,k,i));
163             else
164                 diff(j,k,i) = abs(MR(j,k,i) - Fixed(j,k,i));
165             end
166         end
167     end
168 end
169 end
170 %%
171 diff(isnan(diff)) = 0;
172 se = strel('disk',1);
173 for i = 1:5
174     test = diff(:,:,i);
175     IR = imerode(test,se);
176     diff(:,:,i) = IR;
177     diffc(:,:,i) = diff(:,:,i).*condyles;
178 end

```